

The Bark-Beetle-Associated Fungus, *Endoconidiophora polonica*, Utilizes the Phenolic Defense Compounds of Its Host as a Carbon Source^{1[OPEN]}

Namita Wadke, Dineshkumar Kandasamy, Heiko Vogel, Ljerka Lah, Brenda D. Wingfield, Christian Paetz, Louwance P. Wright, Jonathan Gershenson, and Almuth Hammerbacher^{2*}

Max Planck Institute for Chemical Ecology, 07745 Jena, Germany (N.W., D.K., H.V., C.P., L.P.W., J.G., A.H.); University of Potsdam, 14476 Golm, Germany (L.L.); and Department of Genetics, Forestry and Agricultural Biotechnology Institute, University of Pretoria, Pretoria 0028, South Africa (B.D.W.)

ORCID IDs: 0000-0003-4988-6263 (L.L.); 0000-0001-5998-6079 (L.P.W.); 0000-0002-1812-1551 (J.G.); 0000-0002-0262-2634 (A.H.).

Norway spruce (*Picea abies*) is periodically attacked by the bark beetle *Ips typographus* and its fungal associate, *Endoconidiophora polonica*, whose infection is thought to be required for successful beetle attack. Norway spruce produces terpenoid resins and phenolics in response to fungal and bark beetle invasion. However, how the fungal associate copes with these chemical defenses is still unclear. In this study, we investigated changes in the phenolic content of Norway spruce bark upon *E. polonica* infection and the biochemical factors mediating these changes. Although genes encoding the rate-limiting enzymes in Norway spruce stilbene and flavonoid biosynthesis were actively transcribed during fungal infection, there was a significant time-dependent decline of the corresponding metabolites in fungal lesions. In vitro feeding experiments with pure phenolics revealed that *E. polonica* transforms both stilbenes and flavonoids to muconoid-type ring-cleavage products, which are likely the first steps in the degradation of spruce defenses to substrates that can enter the tricarboxylic acid cycle. Four genes were identified in *E. polonica* that encode catechol dioxygenases carrying out these reactions. These enzymes catalyze the cleavage of phenolic rings with a vicinal dihydroxyl group to muconoid products accepting a wide range of Norway spruce-produced phenolics as substrates. The expression of these genes and *E. polonica* utilization of the most abundant spruce phenolics as carbon sources both correlated positively with fungal virulence in several strains. Thus, the pathways for the degradation of phenolic compounds in *E. polonica*, initiated by catechol dioxygenase action, are important to the infection, growth, and survival of this bark beetle-vectored fungus and may play a major role in the ability of *I. typographus* to colonize spruce trees.

Norway spruce (*Picea abies*), an ecologically and economically important conifer in European boreal and mountainous regions, is susceptible to attack by the bark beetle *Ips typographus* after abiotic stress. This insect species kills mature Norway spruce trees by mass attack using aggregation pheromones to attract conspecifics (Wermelinger, 2004; Kausrud

et al., 2012; Schiebe et al., 2012). Bark beetles are associated with various species of blue-staining ascomycete fungi that are introduced into the host during an attack (Kirisits, 2010). These blue-stain fungi ultimately grow into the cambium and sapwood of trees, where they occlude the vascular bundles and negatively affect wood quality (Kuroda, 2005). Under severe infestation, this can lead to tree mortality. Fungal infestation is hypothesized to enhance bark beetle brood development by exhausting the tree's defenses at an early stage during host colonization (Paine et al., 1997; Krokene and Solheim, 1998, 2001; Nagy et al., 2004; Franceschi et al., 2005; Zhao et al., 2011).

Norway spruce defenses include many different chemical compounds that are thought to protect from insect damage and microbial infection. The best studied chemical defense in this tree species are oleoresins, a blend of monoterpenoids, sesquiterpenoids, and diterpenoids, stored in specialized resin ducts (Keeling and Bohlmann, 2006). Another well-studied class of defenses are phenolic substances, including stilbenes, flavonoids, and proanthocyanidins, that are stored in concentric

¹ This work was supported by the Jena School of Microbial Communication and the Max Planck Society (to J.G., N.W., and A.H.).

² Present address: Department of Microbiology, Forestry and Agricultural Biotechnology Institute, University of Pretoria, Private Bag X20, Pretoria 0028, South Africa.

* Address correspondence to ahammerbacher@ice.mpg.de.

The author responsible for distribution of materials integral to the findings presented in this article in accordance with the policy described in the Instructions for Authors (www.plantphysiol.org) is: Almuth Hammerbacher (ahammerbacher@ice.mpg.de).

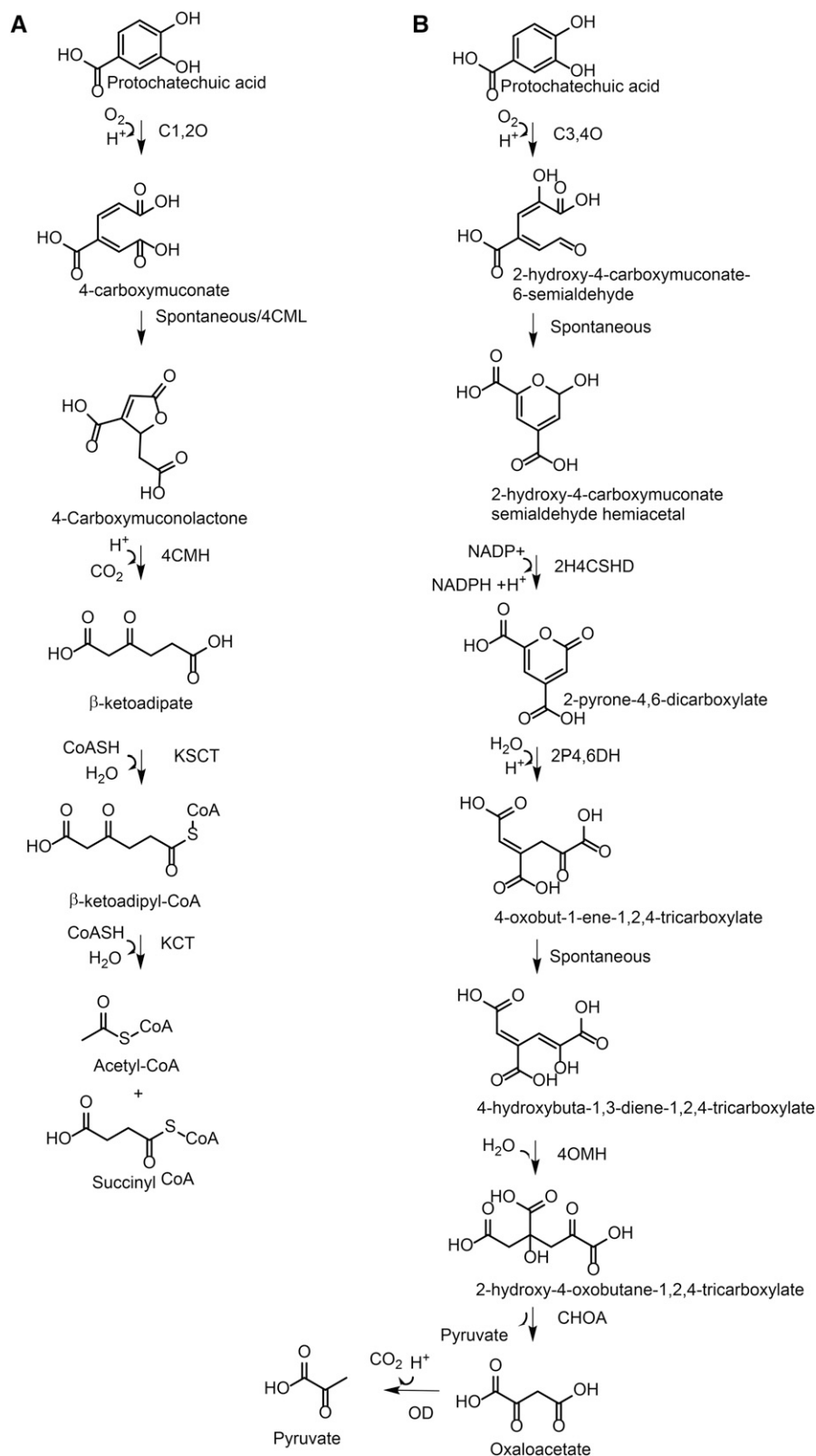
A.H., J.G., and L.P.W. conceived the study and procured funding; N.W., D.K., C.P., H.V., and A.H. did the experiments; B.D.W. and L.L. contributed sequencing data; L.L. constructed the phylogeny; A.H., L.P.W., and J.G. wrote the article.

[OPEN] Articles can be viewed without a subscription.

www.plantphysiol.org/cgi/doi/10.1104/pp.15.01916

rows of phloem parenchyma cells (also known as polyphenolic parenchyma cells) in spruce bark (Li et al., 2012). It has been shown that concentrations of both terpenoids

and phenolics increase in spruce bark upon wounding or fungal infection (Martin et al., 2002; Hammerbacher et al., 2011, 2014).



The mechanisms by which blue-stain fungi exhaust spruce chemical defenses are just beginning to be studied. Both terpenoids and phenolics are present at high concentrations in healthy spruce bark and also are synthesized *de novo* upon mechanical damage and fungal infection (Martin et al., 2002; Hammerbacher et al., 2011, 2014). Recently, astringin, a stilbene glycoside present in the concentric rows of phloem parenchyma cells, was shown to be catabolized by *Endoconidiophora polonica* (Hammerbacher et al., 2013). *E. polonica* (formerly known as *Ceratocystis polonica*; de Beer et al., 2014) is the most virulent blue-stain fungus transmitted by *I. typographus* (Krokene and Solheim, 1998). Although spruce trees still actively synthesize astringin in fungus-infected bark, a net loss of this compound occurs within the fungal lesions (Hammerbacher et al., 2013). This reduction in astringin was attributed to fungal biotransformation processes, including the formation of astringin dimers, aglycones, and ring-cleavage products with muconoid carbon skeletons, but specific genes or enzymes involved in these processes were not identified. It also has been reported that *Grosmannia clavigera*, a blue-stain fungus associated with the mountain pine beetle, could metabolize the oleoresin monoterpene defenses of pine trees (*Pinus* spp.) by oxidative conversion (Wang et al., 2014).

Astringin-derived muconoids may represent the first step of a catabolic pathway for the utilization of aromatic compounds as a carbon source by blue-stain fungi in spruce, similar to the catabolic pathways described for the degradation of small aromatic compounds by soil-dwelling bacteria and fungi (Fig. 1; Harwood and Parales, 1996; Vaillancourt et al., 2006). The first step in the catabolism of simple 3,4-dihydroxylated (catecholic) phenolic compounds by soil microbes is the production of ring-cleaved muconoid derivatives, which is catalyzed by dioxygenase enzymes. Intradiol dioxygenases cleave 3,4-dihydroxylated aromatic rings between the two hydroxyl groups to produce a muconolactone, which is further transformed to β -keto adipate. After activation by two CoA molecules, β -keto adipate is finally processed to form acetyl-CoA and succinyl-CoA. Extradiol dioxygenase enzymes cleave the 3,4-dihydroxylated aromatic ring adjacent to the two hydroxyl groups of the substrate to produce a muconate semialdehyde, which is further transformed to a range of organic acids including pyruvate and oxaloacetate. Products of both pathways are then utilized by the tricarboxylic acid cycle for the production of energy-rich NADH and CO₂. These pathways have special significance in nature and human society due to their involvement in the degradation of the phenolic biopolymer lignin as well as soluble phenolics in litter and other organic waste (Dashtban et al., 2009; Gall et al., 2014). It would be interesting to determine if plant pathogens growing on hosts containing high concentrations of phenolics also employ such pathways for phenolic degradation and exploitation as energy sources. Blue-stain fungi harboring these pathways could potentially be of use as bioremediators of waste affluent from pulp mills or could be exploited to degrade phenolic waste from other industrial processes.

The degradation of phenolic compounds plays a vital role in the survival, growth, and virulence of plant pathogens on various herbaceous (El Hadrami et al., 2015; Lowe et al., 2015) and woody (Hammerbacher et al., 2013) host plants. Here, we continue our investigation of phenolic degradation in *E. polonica*, a blue-stain fungus transmitted by bark beetle attack. Not only stilbenes but also flavonoids were found to be degraded in Norway spruce bark. We isolated transcripts encoding catechol dioxygenases, enzymes with a broad substrate range that catalyze the first step in phenolic catabolism by *E. polonica*, converting stilbenes and flavan-3-ols to ring-cleaved muconoid products.

RESULTS

Changes in Phenolic Biosynthesis and Accumulation in Norway Spruce Bark after *E. polonica* Infection

In order to analyze the phytochemical changes in Norway spruce after inoculation with the bark beetle-associated fungus *E. polonica*, 12-year-old spruce saplings were wounded and inoculated with two fungal strains differing in virulence (less virulent isolate [AV] and virulent isolate [V]; Hammerbacher et al., 2013; Table I). Controls included unwounded saplings and those subjected to wounding without fungal inoculation. Lesions created in spruce bark by the fungus 28 d after inoculation were sectioned to separate the inner lesion close to the inoculation point from the expanding outer part of the lesion, where the fungus had just started to colonize the host tissue. The expression of genes encoding key enzymes in the biosynthesis of stilbenes and flavonoids was analyzed in the separated lesion sections.

The gene expression of stilbene synthase (STS; Hammerbacher et al., 2011), the key enzyme in stilbene biosynthesis in Norway spruce, increased significantly in response to infection by both *E. polonica* isolates at the inoculation site as well as in the expanding lesion compared with the wounded but uninoculated control ($P = 0.04$; Fig. 2). A 2-fold increase was observed in STS transcript abundance at the inoculation site in response to both fungi, but a 4-fold increase could be documented in the expanding lesion in response to infection by V. Values for the unwounded control saplings were 3-fold lower than for the wounded but uninoculated controls (data not shown). In contrast to the elevated STS gene expression after fungal infection, the levels

Table 1. Lesion lengths induced by V and AV *E. polonica* compared with the phloem discoloration observed in spruce saplings that were wounded but not inoculated

Sample	Lesion Length mm
Wounded control	9.1 ± 2.3
V	77.3 ± 19.3
AV	34.9 ± 6.1

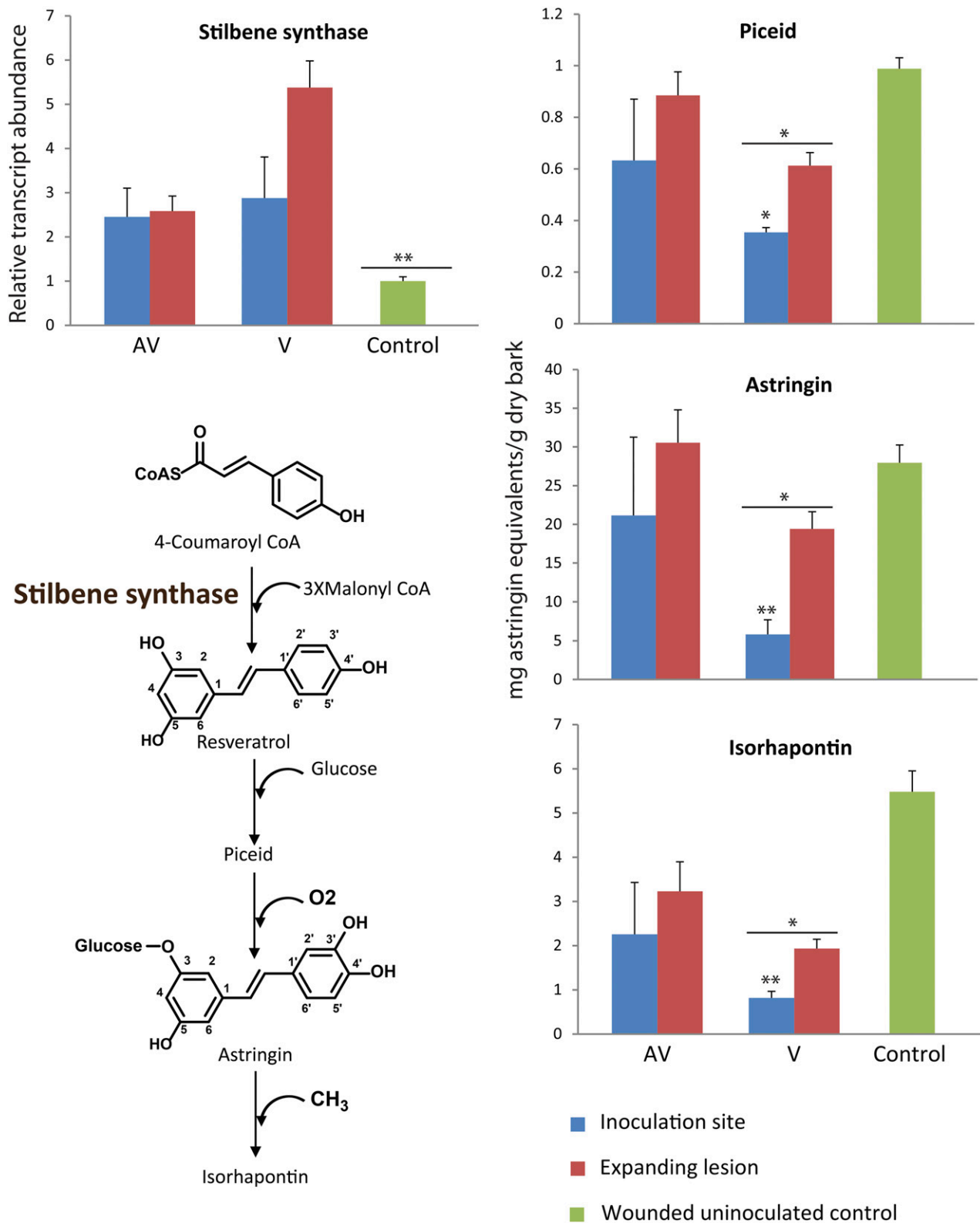


Figure 2. Stilbene biosynthesis of Norway spruce in response to infection by AV and V strains of *E. polonica*. Expression of the gene encoding the rate-limiting enzyme in this pathway, STS, increased in response to fungal infection. Piceid, astringin, and isorhapontin accumulated in wounded but uninfected control bark and in bark infected by AV but declined in bark infected by V at the site of initial bark colonization (inoculation site) and at the edges of the fungal lesion (expanding lesion). Error bars represent

of the stilbene glucosides piceid, astringin, and isorhapontin observed in the fungal lesions were generally lower than those in the wounded but uninoculated controls. These reduced metabolite levels were most evident at the inoculation site ($P = 0.04$ for piceid, $P = 0.004$ for astringin, and $P = 0.003$ for isorhapontin) and to a lesser degree in the expanding lesion of V. Metabolite levels differed significantly in lesions induced by V compared with AV and the wounded control ($P = 0.05$ for piceid, $P = 0.01$ for astringin, and $P = 0.02$ for isorhapontin). Stilbene concentrations also were lower in the inner lesions induced by AV compared with the bark of control saplings, but these differences were not statistically significant (Fig. 2).

Chalcone synthase (CHS) encodes an enzyme family catalyzing the rate-limiting step in flavonoid biosynthesis (Hammerbacher et al., 2014). Similar to STS gene expression, transcript accumulation of CHS increased by more than 3-fold in the lesion sections of V ($P = 0.05$) and to 1.5-fold in the expanding lesion of AV ($P > 0.05$; Fig. 3) compared with the levels of CHS transcript in wounded but uninoculated control saplings. Naringenin, the direct product of CHS, is oxidized in two enzymatic steps to form the dihydroflavonol, taxifolin, that occurs in high concentrations in nonwounded spruce bark. In our experiment, lower levels of this compound were detected in fungus-infected bark sections than in the wounded control sections ($P = 0.01$). Especially in the inner lesion of V close to the inoculation point, a very strong decrease in taxifolin was observed ($P = 0.005$). Taxifolin also serves as a substrate for the biosynthesis of other flavonoids in Norway spruce and is reduced in two NADPH-dependent reduction steps to the flavan-3-ol catechin, which is subsequently polymerized to the flavan-3-ol dimer, PA B1 (Hammerbacher et al., 2014). Both catechin and PA B1 content declined in the inner lesions induced by AV and V ($P < 0.001$ for catechin and $P = 0.1$ for PA B1) compared with the expanding lesions and the wounded controls ($P < 0.05$). However, catechin levels increased in the expanding lesion of AV and PA B1 content increased in the expanding lesions of both fungal isolates when compared with the wounded control, although these increases were only significant for the nonvirulent isolate ($P < 0.01$ for catechin and $P = 0.04$ for PA B1; Fig. 3).

Taken together, these results show that, although the genes encoding the rate-limiting enzymes in stilbene and flavonoid biosynthesis are actively transcribed during fungal infection, there are significant declines in stilbene and flavonoid metabolites in the lesions created during infection by *E. polonica*. This decline was highest in the inner lesions close to the inoculation site. A comparison of the lesions of the two *E. polonica* isolates

clearly showed that, while the transcription of genes involved in polyphenol biosynthesis was more active in response to V, metabolite levels were lower in the lesions created by this fungus compared with those from the lesions created by AV.

Biotransformation of Astringin and Catechin by *E. polonica* in Vitro

To explore the hypothesis that *E. polonica* is directly responsible for the decline of polyphenolic defense metabolites in its spruce host, AV and V were grown in artificial medium supplemented with the stilbene astringin or the flavan-3-ol catechin. The concentrations of both metabolites declined in the medium 12 h after incubation (Fig. 4A), with lower metabolite levels recovered from medium colonized by V ($P = 0.02$ for both metabolites) compared with AV. Biotransformation of catechin by both fungal isolates was lower than that observed for astringin ($P < 0.001$). For both metabolites, muconoid biotransformation products were recovered from the medium (Fig. 4B).

The decline in metabolites in the fungus-colonized artificial medium in this experiment effectively mirrors the metabolite decline observed in infected spruce bark (Figs. 2 and 3). Taken together, these results clearly show that *E. polonica* can metabolize the polyphenolic defense compounds and that the muconoids recovered from *E. polonica*-colonized medium represent catabolites of this process.

Identification and Phylogenetic Analysis of Catechol Dioxygenase Genes in *E. polonica* and Other Blue-Stain Fungi

To identify enzymes in *E. polonica* involved in the catabolism of Norway spruce polyphenols, an EST library of this fungus was sequenced using an Illumina HiSeq 2000 sequencer (MWG Operon). A total of 42 million reads were assembled into approximately 32,000 contigs, from which 12 contigs were highly similar to coding regions of catechol dioxygenase (CDO) genes from GenBank. CDOs are a family of enzymes catalyzing the cleavage of phenolic rings with a vicinal dihydroxyl function. Further analysis showed that these 12 CDO contigs could be reassembled into three partial transcripts and one full-length transcript. The partial open reading frames were then completed using the RACE method. To confirm the identity of these CDO sequences and verify that all CDO transcripts were identified in *E. polonica*, BLAST searches were conducted using the unpublished partial genomes of both *E. polonica* and its closest relative, *Endoconidiophora*

Figure 2. (Continued.)

SE ($n = 5$). Asterisks with bars indicate significant differences between AV, V, and control; asterisks illustrate significant differences between different lesion areas: *, $0.01 < P < 0.05$ and **, $P < 0.01$.

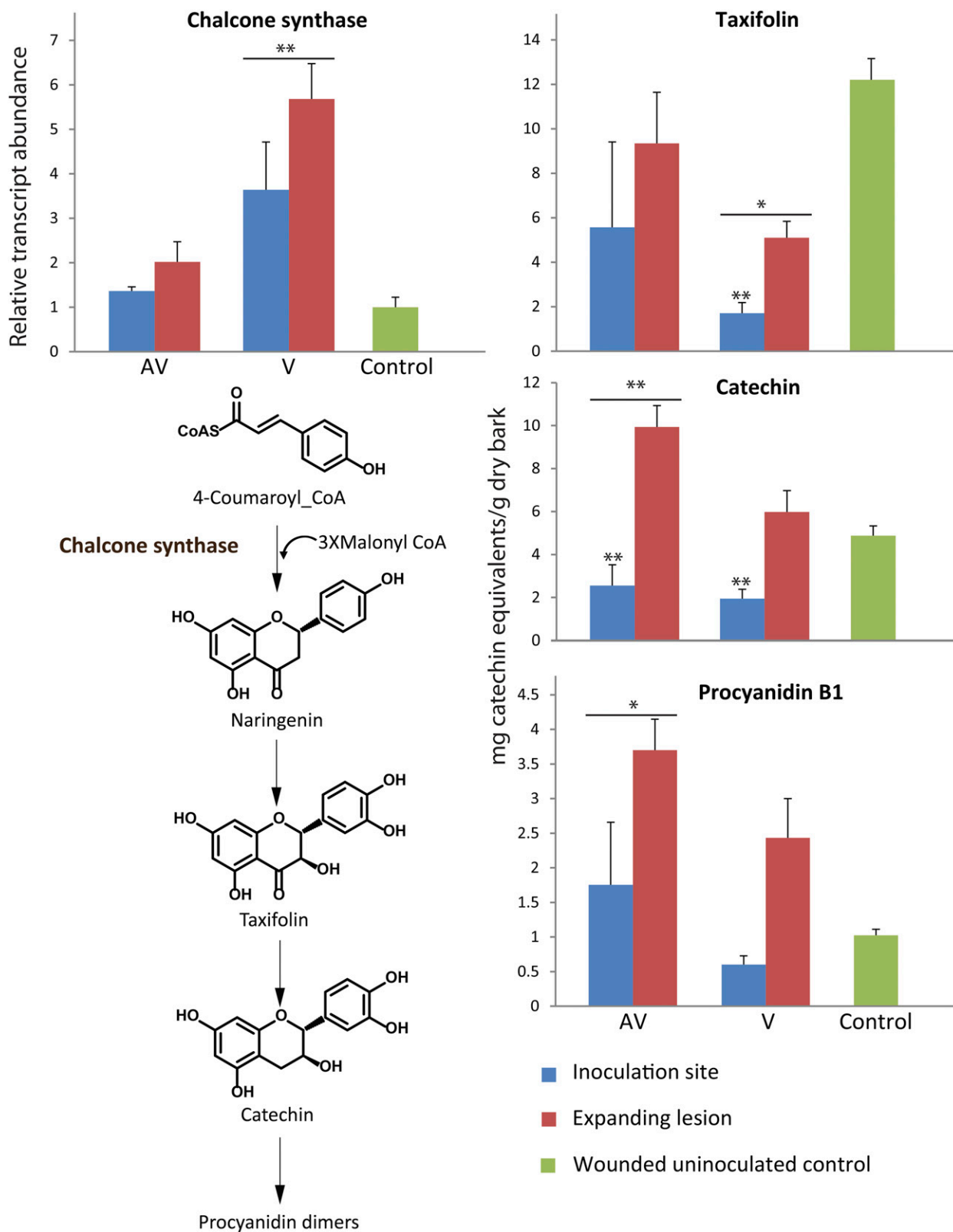


Figure 3. Flavonoid biosynthesis of Norway spruce in response to infection by AV and V *E. polonica* strains. Expression of the gene encoding the rate-limiting enzyme in this pathway, CHS, increased in response to fungal infection. Taxifolin accumulated to high levels in wounded but uninfected control bark but was present at lower concentrations in fungus-infected bark at the site of initial colonization by the fungus (inoculation site) and at the edges of the fungal lesion (expanding lesion). Catechin and

laricicola. Analysis of the four open reading frames for signal peptides revealed that three of the sequences, designated EpCDO1, EpCDO2, and EpCDO3, lack signal peptides and, therefore, encode cytoplasmic enzymes, while EpCDO4 has a secretory signal localizing it to the extracellular space. Furthermore, EpCDO1, EpCDO2, and EpCDO4 encode sequences similar to previously characterized intradiol dioxygenases, while the sequence of EpCDO3 encodes an extradiol dioxygenase (Harwood and Parales, 1996).

A phylogenetic analysis of CDO sequences was conducted at the amino acid level with four species of blue-stain fungi for which adequate information is available. Analysis showed that each *E. polonica* CDO aligns in its own clade with sequences of the other three species. The major evolutionary divisions in this alignment correspond to differences in biochemical functions, with a clear divergence between the two major dioxygenase subfamilies: the extradiol-cleaving dioxygenases (containing the PF02900 domain and including CDO3) and the intradiol dioxygenases (containing the PF00775 domain and including CDO1, CDO2, and CDO4). Within the intradiol subfamily, the extracellular CDO4 diverged earlier in evolution from the line leading to CDO1 and CDO2, which are sister clades.

Within the clades of each *E. polonica* CDO, the positions of the orthologous proteins agree with the accepted species phylogeny of the four fungi, with the exception of CDO2. The genomes of the Sordariomycetidae species included in the analysis, *Ophiostoma novo-ulmi*, *Ophiostoma piceae*, and *G. clavigera*, each have four CDO3 paralogs, two CDO2 and CDO4 paralogs, and only one CDO1. In contrast, the genome of *E. polonica* from the sister subclass Hypocreomycetidae contains only one gene for each of these CDO clades (Fig. 5).

CDO Transcript Abundance in *E. polonica* during Spruce Infection

To gain a better understanding of the involvement of *EpCDO* genes in spruce infection, the transcript abundance of these genes was quantified in infected spruce bark by quantitative real-time-PCR. The transcript abundances of EpCDO1, EpCDO3, and EpCDO4 were significantly higher in the lesions created by V than in the lesions of AV ($P > 0.05$; Fig. 6). In V, EpCDO1 and EpCDO3 were expressed at similar levels in both the inner lesion sections and the expanding lesions, while EpCDO4 was expressed at significantly higher levels in the expanding lesions ($P = 0.03$). EpCDO2 was

expressed at similar levels in the inner and expanding lesions of both isolates.

Characterization of EpCDO Enzyme Activities and Substrate Specificity

The four full-length EpCDO transcripts were subcloned into the expression vector pH9 (Yu and Liu, 2006) and heterologously expressed in *Escherichia coli*. After purification, the enzymes were offered the universal CDO substrate catechol under different reaction conditions and the products were identified by liquid chromatography-mass spectrometry (LC-MS). Optimum enzyme activity was attained at pH 7.5, 30°C, and 0.05 mM of the cofactor FeCl₃ (or FeCl₂ for EpCDO3). A range of different substrates from spruce and products of fungal metabolism were used to test the substrate specificity of CDO enzymes from *E. polonica* (Table II). As expected, EpCDO enzymes accepted substrates containing a vicinal dihydroxyphenol group such as catechol, caffeic acid, and astringin to produce the corresponding muconolactone or muconate semialdehyde products (Fig. 1). 4-Hydroxyphenolic compounds without a second adjacent hydroxyl function, such as *p*-coumaric acid or piceid, as well as 3-methoxy-4-hydroxyphenols were not accepted. EpCDO enzymes accepted even complex phenolic compounds such as the flavan-3-ols catechin and PA B1 as long as these had a vicinal dihydroxyl group. However, taxifolin, a dihydroflavonol present in spruce bark with a vicinal dihydroxyl group that declines during *E. polonica* infection, was not accepted as a substrate. The Trp degradation product dihydroxy-Phe was only accepted by the extradiol dioxygenase EpCDO3.

After these substrate and product surveys, EpCDO enzymes were characterized in detail by determining their catalytic efficiencies using catechol, the standard substrate for this enzyme class, and three other substrates representing the major categories of phenolics encountered by the fungus during its life cycle in spruce bark: caffeic acid, a phenolic acid; astringin, a stilbene glycoside; and catechin, a flavan-3-ol (Table III). EpCDO1 had the highest catalytic efficiency (k_{cat}/K_m) with catechol, compared with the other substances, and also was effective in oxidizing catechin and astringin to the corresponding muconolactones. EpCDO2, which was constitutively expressed by both fungi in all lesion sections, was highly efficient in transforming all four substrates into muconolactone products. The extradiol dioxygenase EpCDO3, the only enzyme that accepted dihydroxy-Phe as a substrate, showed

Figure 3. (Continued.)

procyanidin B1 (PA B1) concentrations increased in the expanding lesion of fungus-infected tissue compared with the control. Error bars represent se ($n = 5$). Asterisks with bars illustrate significant differences between AV, V, and control; asterisks illustrate significant differences between different lesion areas: *, $0.01 < P < 0.05$ and **, $P < 0.01$.

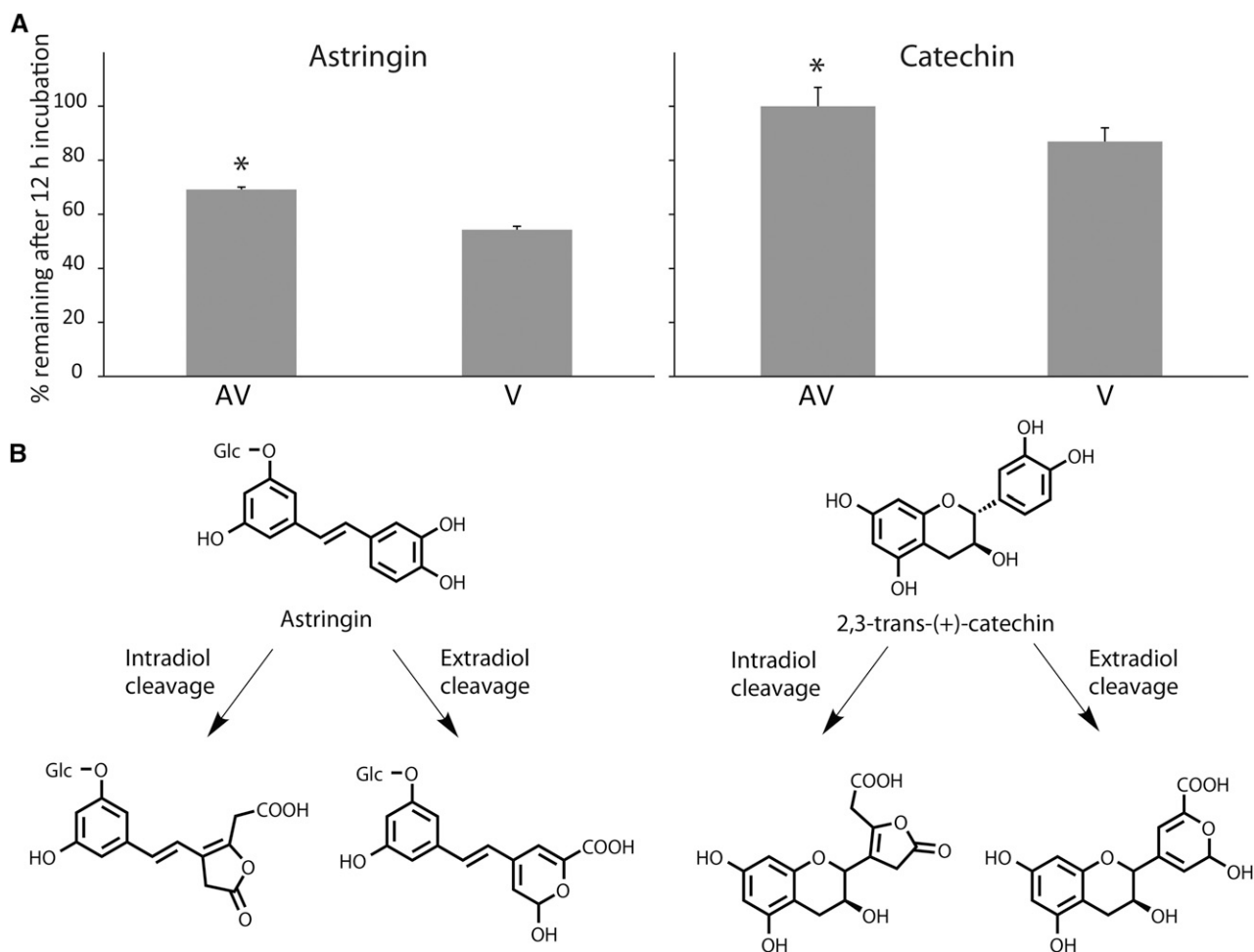


Figure 4. *E. polonica* metabolizes spruce phenolics offered in artificial growth medium and transforms them to muconates. A, Percentage astringin and catechin remaining in liquid potato dextrose medium after 12 h of incubation at 24°C with shaking at 60 rpm. Controls without fungus showed no significant losses of phenolic metabolites ($n = 5$; error bars represent SE; *, $P = 0.02$). B, Chemical structures of muconate derivatives of astringin and catechin that accumulated in the medium.

low catalytic efficiencies for catechol and caffeic acid but was very efficient in catalyzing the conversion of astringin and to a lesser extent catechin to their respective muconate semialdehydes. The extracellularly localized EpCDO4 was less efficient in converting catechol, astringin, and catechin to muconolactones than the other enzymes, but it accepted caffeic acid more readily as a substrate than EpCDO1 and EpCDO3.

Correlation between Virulence and Fungal Utilization of Polyphenols

EpCDO enzymes catalyze the first step in the degradation of phenolic compounds, a process that may serve not only to detoxify host defenses but also to provide a carbon source for growth (Hammerbacher et al., 2013). To study the importance of these pathways

for *E. polonica*, the growth of different isolates of this species in living spruce was quantified and compared with the growth rate on minimal medium amended with astringin or catechin as carbon source. There was a significant positive correlation of the in vitro growth rates of eight *E. polonica* isolates on both astringin and catechin with their relative virulence (Fig. 7). A four-parameter exponential function gave the best fit, with $r^2 = 0.97$ ($P < 0.05$) for catechin and $r^2 = 0.63$ ($P < 0.05$) for astringin.

DISCUSSION

Blue-stain fungi are often inoculated into conifer trees by attacking bark beetles, but their role in promoting bark beetle colonization is not well understood. Here, we demonstrate that a blue-stain fungus degrades the major phenolic compounds of its host tree by a catabolic pathway initiated by oxidative ring cleavage. The

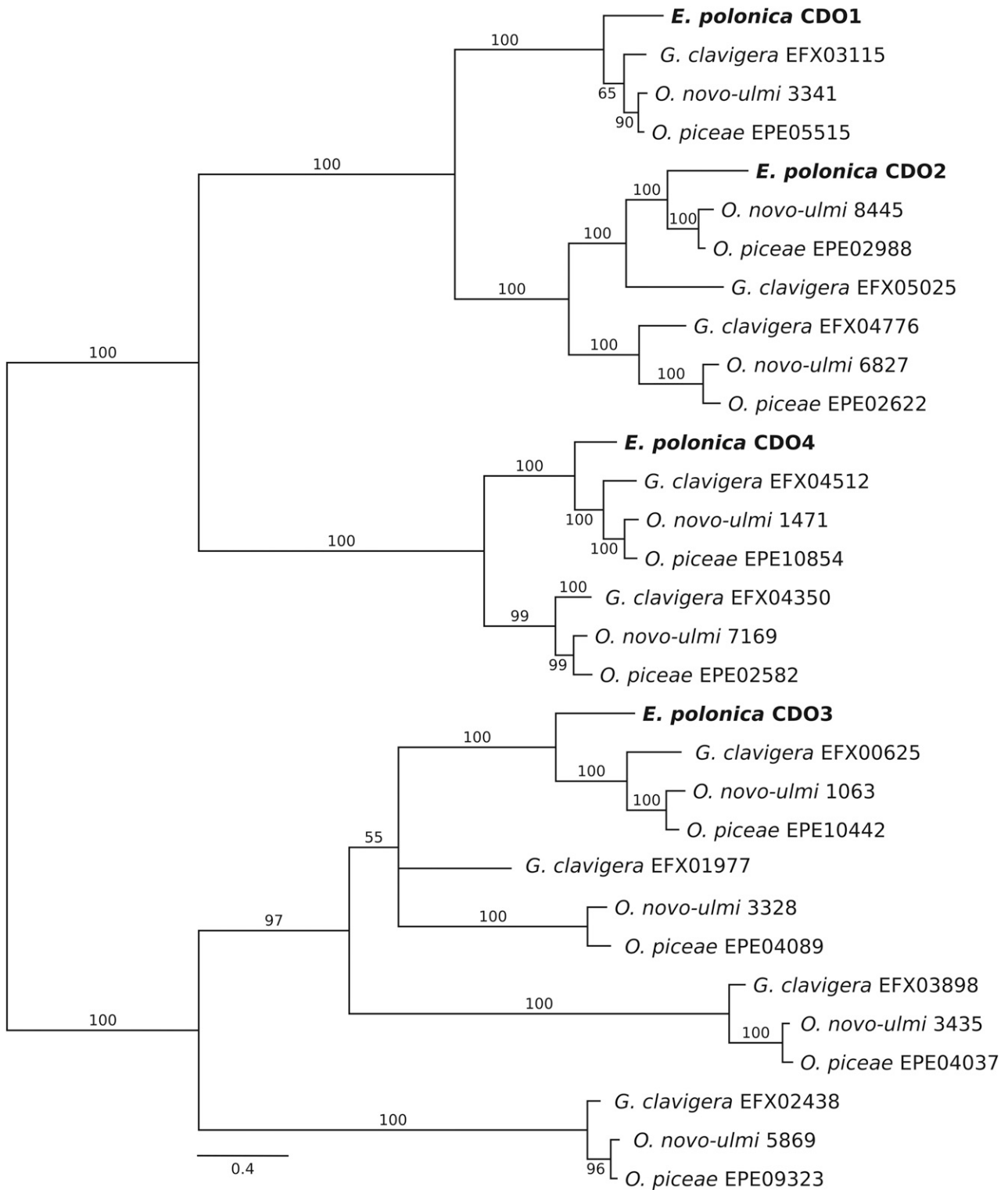


Figure 5. Phylogenetic analysis of CDO proteins from *E. polonica* (Hypocreomycetidae), and *O. piceae*, *O. novo-ulmi*, and *G. clavigera* (Sordariomycetidae). The unrooted Bayesian phylogeny was based on the alignment of CDO homologs retrieved from proteomes of selected species based on conserved protein domains. Clade support values are given as Bayesian posterior probabilities in percentages. Branch labels include species names and National Center for Biotechnology Information sequence identifiers. *O. novo-ulmi* identifiers were shortened for simplification and should contain OphioH327gp immediately before the four-digit identifier.

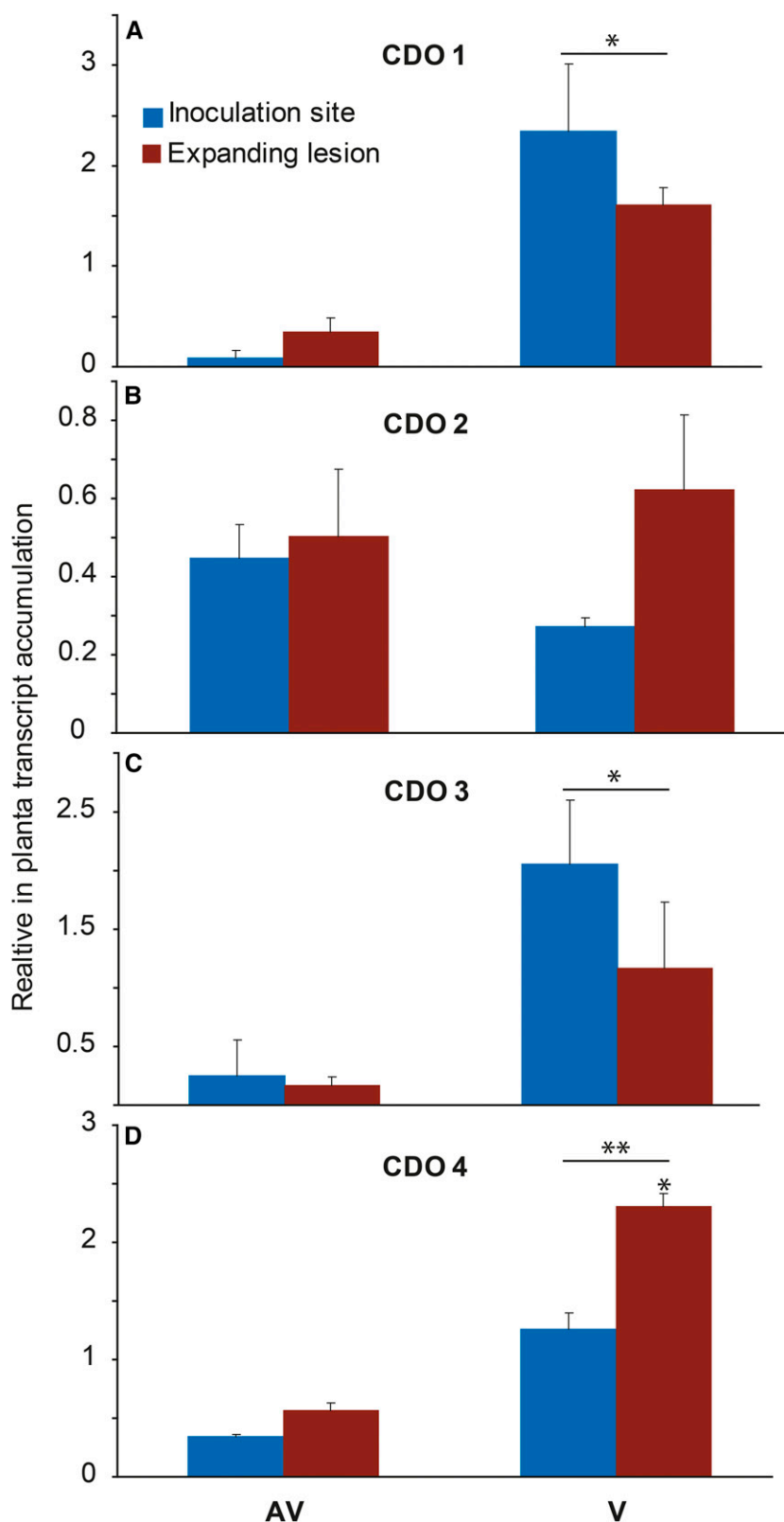


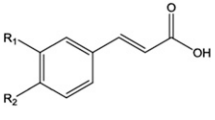
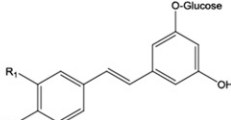
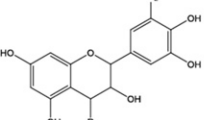
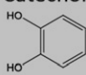
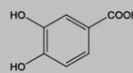
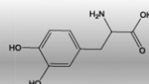
Figure 6. Relative gene expression of *E. polonica* CDO genes in infected Norway spruce bark at the site of initial bark colonization and at the edges of the fungal lesion for both AV and V strains. EpCDO transcript accumulation was determined using quantitative real-time-PCR and normalized against chitin synthase from *E. polonica*. Asterisks with bars illustrate significant differences between AV, V, and control; asterisks illustrate significant differences between different lesion areas: *, $0.01 < P < 0.05$ and **, $P < 0.01$. Error bars represent se ($n = 5$).

ascomycete *E. polonica*, the most virulent fungal associate of the Eurasian spruce bark beetle *I. typographus*, employs CDOs as a first step in the degradation of

stilbenes and flavan-3-ols in Norway spruce, a process that enhances the growth and survival of the fungus during host infection.

Table II. Substrate specificity of *E. polonica* CDOs for phenolic defense compounds commonly occurring in Norway spruce bark

Shaded cells indicate substrates accepted. Dihydroxy-Phe was only accepted as a substrate by EpCDO3. Recombinant enzymes were tested in vitro with 10 mM substrate and 0.005 mM FeCl₃ (or 0.005 mM FeCl₂ for EpCDO3) in 50 mM Tris buffer, pH 7.5, with 10% glycerol and 1 mM dithiothreitol (DTT).

Phenolic acids	Stilbenes	Flavonoids	Products of general metabolism
			
Coumaric acid R ₁ – H R ₂ – OH	Piceid R ₁ – H R ₂ – OH	Taxifolin R ₁ – O R ₂ – H	Catechol 
Caffeic acid R ₁ – OH R ₂ – OH	Astringin R ₁ – OH R ₂ – OH	Catechin R ₁ – H R ₂ – H	Protocatechuic acid 
Ferulic acid R ₁ – OCH ₃ R ₂ – OH	Isorhapontin R ₁ – OCH ₃ R ₂ – OH	Proanthocyanidin B1 R ₁ – Catechin R ₂ – H	Dihydroxyphenylalanine 

E. polonica Degrades Two Classes of Phenolic Antifungal Defenses during Norway Spruce Infection

Two major classes of soluble polyphenol compounds in spruce bark, stilbenes and flavan-3-ols, have been described to be potent antifungal agents (Chong et al., 2009; Hammerbacher et al., 2014) that interfere with membrane potential (Adrian et al., 1998), electron transport (Pont and Pezet, 1990), melanin biosynthesis, and the formation of structures used by fungi to penetrate their hosts (Chen et al., 2006). Furthermore, polyphenols are antinutritional to microbes, since they chelate metals, precipitate proteins and other nutrients, and bind to extracellular digestive enzymes, rendering them nonfunctional (for review, see Scalbert, 1991). After infection by *E. polonica* in our study, the transcription of Norway spruce transcripts encoding key enzymes in the biosynthesis of stilbenes and flavan-3-ols was significantly up-regulated, suggesting that spruce actively produces stilbenes and flavonoids in response to fungal infection. In previous studies on Norway spruce or *Picea glauca*, the transcript abundances of STS and CHS genes or the activities of the encoded enzymes also increased after inoculation with *E. polonica* (Brignolas et al., 1995; Hammerbacher et al., 2011, 2014).

However, despite the increases in stilbene and flavonoid biosynthesis observed here upon *E. polonica* infection, we recorded a significant decline in the content of these metabolites in fungus-infected spruce bark tissue. By separating the fungal lesion into two parts, (1) the inner lesion, where fungal colonization of the bark tissue was complete, and (2) the outer lesion, where

colonization was still in progress, we showed that the decline in metabolites was most extensive in the inner lesion surrounding the inoculation point. In vitro feeding experiments with pure stilbenes and flavan-3-ols confirmed that *E. polonica* can metabolize these compounds. The most abundant biotransformation products produced in cultures of a virulent *E. polonica* strain were muconoid-type derivatives of the stilbene astringin and the flavan-3-ol catechin (Fig. 4). Astringin was found previously to be metabolized by both V and AV *E. polonica* to various other products, including aglucones as well as dimers that were shown to accumulate in vitro (Hammerbacher et al., 2013) as well as in vivo (Viiri et al., 2001; Li et al., 2012).

E. polonica Employs CDOs to Cleave the 3,4-Hydroxy Rings of Spruce Phenolics

In a previous study, we showed that muconoid production from astringin was the preferred stilbene biotransformation strategy of a virulent *E. polonica* strain (Hammerbacher et al., 2013). It was not known, however, if other abundant spruce polyphenols also are transformed by this fungus in a similar way. In this study, we showed that *E. polonica* also can transform the 3,4-hydroxyphenols of other abundant spruce polyphenols such as catechin, PA B1, and caffeic acid into muconoids.

The formation of muconoids is a well-described biotransformation strategy of soil bacteria and fungi for the degradation of simple phenolic compounds such as catechol and protocatechuic acid (Harwood and

Table III. Kinetic parameters for *E. polonica* CDOs for substrates representing each of the major classes of phenolics in spruce bark

K_m is the substrate concentration where the enzyme reaction speed is half of the maximum reaction speed, V_{max} ; k_{cat} is the maximum number of molecules that are turned over by an enzyme per second; k_{cat}/K_m is the catalytic efficiency of an enzyme.

Substrate	Enzyme	K_m	k_{cat}	k_{cat}/K_m
		<i>mM</i>	<i>s</i> ⁻¹	
Catechol	CDO1	0.087	4.873	56.029
	CDO2	0.088	2.419	27.371
	CDO3	9.587	2.890	0.301
	CDO4	0.960	0.234	0.244
Caffeic acid (a phenolic acid)	CDO1	0.137	0.175	1.280
	CDO2	0.044	0.549	12.533
	CDO3	1.063	4.636	4.364
	CDO4	0.116	1.298	11.175
Astringin (a stilbene)	CDO1	0.057	0.461	8.102
	CDO2	0.040	0.737	18.458
	CDO3	0.121	4.391	36.367
	CDO4	0.065	0.338	5.210
Catechin (a flavan-3-ol)	CDO1	2.628	31.749	12.079
	CDO2	1.821	33.956	18.647
	CDO3	4.684	61.738	13.181
	CDO4	0.614	4.199	6.837

Parales, 1996). The cleavage of dihydroxylated aromatic rings is known to be catalyzed by CDO enzymes acting in an extradiolitic or intradiolitic fashion (Fig. 1). The muconoid products are transformed subsequently via a number of enzymatic steps into substrates of the tricarboxylic acid cycle, which are then catabolized further to CO₂ with the additional production of energy-rich NADH (Harwood and Parales, 1996).

Our Bayesian phylogenetic analysis of CDO sequences in blue-stain fungi provides an evolutionary framework for functional specialization as well as CDO family expansion with lineage diversification. We identified four CDO transcripts in an *E. polonica* (subclass Hypocreomycetidae of the class Sordariomycetes, division Ascomycota) EST library and retrieved CDO homologs from the genomes of *O. piceae*, *O. novo-ulmi*, and *G. clavigera* (subclass Sordariomycetidae of the class Sordariomycetes). Two major CDO clades were apparent that reflect differences in the functional protein domain present and corresponding differences in the phenolic ring cleavage mechanisms, either extradiol (CDO3) or intradiol (CDO1, CDO2, and CDO4) cleavage (Vaillancourt et al., 2006).

Within these major CDO clades, the branching generally agrees with accepted species phylogenies. The presence of CDO2, CDO3, and CDO4 paralogs within Sordariomycetidae species, but not *E. polonica* from the sister Hypocreomycetidae clade, can be explained by two alternative evolutionary scenarios: either the last common ancestor of Hypocreomycetidae and Sordariomycetidae possessed only the four CDO1 to CDO4 genes still present in *E. polonica* followed by lineage-specific expansions in the Sordariomycetidae, or the specific CDO paralogs were lost in *E. polonica*. Gene

loss in this case could indicate a high degree of specialization of the fungus to its host, with retention of only the genes necessary for its survival in spruce bark. This latter, more parsimonious, scenario would suggest the presence of paralogs already in the last common ancestor of both subclasses as well as in other taxa and species found in the two subclasses.

In support of this second scenario, the genome of the generalist *Glomerella cingulata* (Hypocreomycetidae; Gan et al., 2013) has 17 genes coding for intradiol CDOs. A preliminary phylogenetic analysis (data not shown) suggests that these genes are spread among all three intradiol CDO clades as orthologs of Sordariomycetidae genes and also represent lineage- or species-specific expansions, especially in the CDO4 clade. *G. cingulata* causes anthracnose disease in a number of herbaceous hosts, which often contain high levels of soluble phenolics such as flavan-3-ols, flavonoids, and caffeoylquinic acids (Cheynier, 2012). The high number of CDO genes in the *G. cingulata* genome thus suggests that this strategy of degrading plant phenolic defense compounds is not limited to fungi infecting woody hosts but also seems to

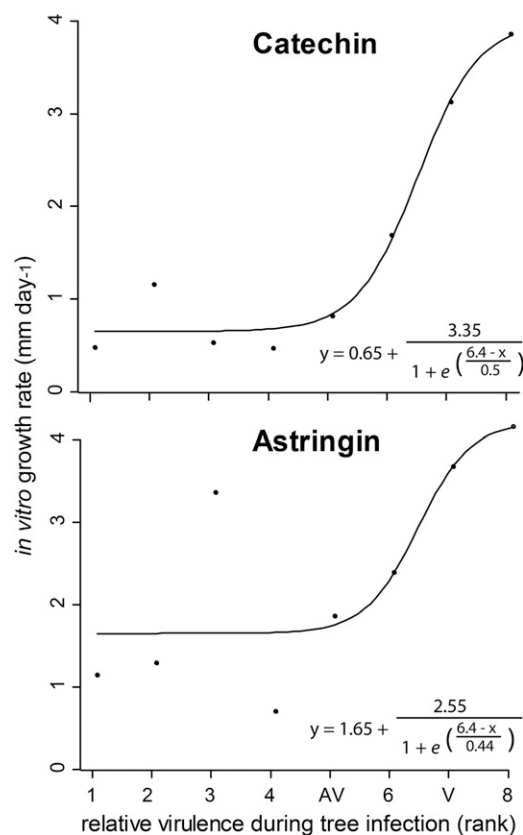


Figure 7. Growth of eight *E. polonica* strains on astringin or catechin as sole carbon source in artificial medium correlated with their ranked virulence during tree colonization when plotted on a four-parameter regression function (nonlinear regression analysis: catechin, $r^2 = 0.97$ and astringin, $r^2 = 0.63$). Virulence was determined by measurements of lesion lengths of infected *P. glauca* saplings.

be a common trait of plant pathogenic fungi infecting herbaceous species.

The heterologously expressed *EpCDO* genes all accepted catechol and protocatechuic acid as substrates and also converted more complex phenolic compounds such as caffeic acid, astringin, catechin, and procyanidin dimers to muconoid products. Interestingly, although these enzymes readily accepted complex flavan-3-ols, such as PA B1, as substrates, they could not convert flavonols and dihydroflavonols to the respective muconoids. Thus, the depletion of the dihydroflavonol taxifolin in spruce bark colonized by *E. polonica* is not due to the direct action of CDO enzymes. *E. polonica* might thus use an alternative biodegradation strategy for taxifolin, for example starting with an initial cleavage of the C-ring and further degradation to protocatechuic acid, as has been described for *Pseudomonas putida* (Pillai and Swarup, 2002).

As expected, *EpCDO* enzymes also did not cleave any compounds lacking 3,4-dihydroxylated rings, such as the stilbenes, piceid, and isorhapontin. Yet, the concentrations of these compounds also were significantly lowered in fungus-infected bark, indicating that *E. polonica* must have other biotransformation strategies to catabolize these phenolic rings. For example, it has been shown that *E. polonica* can polymerize stilbenes to form compounds that are less soluble in aqueous solution (Hammerbacher et al., 2013). Alternatively, a 3,4-dihydroxyl function in a phenolic ring system can be formed in situ from other substitution patterns, yielding compounds that are then subject to extradiol or intradiol cleaving CDOs. For example, bacteria have been shown to demethylate the methoxyl functions in compounds such as vanillin to yield dihydroxylated products that can serve as substrates for ring-opening dioxygenases (Chen et al., 2012; Lowe et al., 2015). A similar process could be involved in the degradation of ferulic acid and isorhapontin. Furthermore, microbes can oxidize unsubstituted phenolic rings such as that of benzoic acid to form a 3,4-dihydroxylated product suitable for CDO cleavage (Suenaga et al., 2009). The oxidation of phenolic rings might thus play an important role in the catabolism of resveratrol or coumaric acid by *E. polonica*.

When the rate of reaction for *EpCDO* enzymes was compared using a range of different substrates that might be encountered by the fungus during its life cycle in Norway spruce, *EpCDO1* was found to be highly efficient in transforming catechol to muconolactone, but it had lower catalytic efficiencies for transforming more complex phenolics. This suggests that this enzyme is similar to the CDO enzymes described for *Pseudomonas* spp., which have narrow substrate specificities and high catalytic efficiencies for transforming a single substrate (Pillai and Swarup, 2002). The intradiol-cleaving *EpCDO2*, on the other hand, had very broad substrate specificity, as it effectively transformed a range of polyphenols to the corresponding ring-opened lactones. The extradiol-cleaving *EpCDO3*, which also accepted the nitrogenous compound

dihydroxy-Phe, had a low catalytic efficiency for catechol and caffeic acid but was extremely efficient in utilizing astringin and catechin. As *EpCDO1*, *EpCDO2*, and *EpCDO3* are localized in the cytoplasm of *E. polonica*, they also might be involved in the catabolism of cellular constituents such as aromatic amino acids (e.g. dihydroxy-Phe). Their ability to effectively transform and detoxify defense-related polyphenols that diffuse into the cell and that may interfere with fungal metabolism and ultimately growth might represent a very important fungal adaptation for survival in polyphenol-rich Norway spruce bark tissue. This hypothesis is further supported by the fact that genes encoding *EpCDO1*, *EpCDO2*, and *EpCDO3* were expressed at similar levels at the inoculation site and the expanding lesions.

EpCDO4 was the only enzyme from *E. polonica* with a signal peptide localizing it to the extracellular space. This enzyme preferentially accepted the phenolic acid, caffeic acid, which in its methylated and reduced form is an important component of conifer lignin. Blue-stain fungi grow from their initial point of infection in the bark into the wood of conifer trees (Krokene and Solheim, 2001). Therefore, it is possible that *EpCDO4* is involved in the catabolism of accessible cell wall constituents in the wood and plays a role in fungal penetration and colonization of woody tissue together with other oxidative processes. The *EpCDO4* gene was expressed by *E. polonica* at higher levels in the expanding lesions than in the inner lesion, which also supports its hypothetical role in fungal colonization of woody tissue.

To compare the substrate usage of CDOs, we quantified assay products by LC-MS methods rather than measuring the consumption of catechol substrate colorimetrically (Gulvik and Buchan, 2013) or the consumption of oxygen using a Clarke electrode (Haigler et al., 1992), as has sometimes been done previously. However, determining the kinetic parameters of these enzymes is complicated by the tendency of phenolic substrates to precipitate proteins under acidic conditions or to attack nucleophilic amino acid residues of the protein under basic conditions, leading to an overestimation of the concentration of active protein in the assay. Polyphenols also chelate the iron cofactor of *EpCDO* enzymes in the reaction mix, which influences cofactor concentrations as well as the concentrations of soluble phenolic substrates in the assay. However, even if the kinetic parameters are not completely exact, we believe that our results give an accurate estimation of the differences in substrate specificity among the different CDO types.

Degradation of Spruce Phenolics Is an Important Virulence Factor for *E. polonica* during Tree Infection and Colonization

It was shown recently that polyphenol catabolism is of great importance for both the bacterium *Ralstonia*

solanacearum (Lowe et al., 2015) and the fungus *Verticillium dahliae* (El Hadrami et al., 2015) in gaining entry into their herbaceous plant hosts as well as in detoxifying defenses. Our study presents evidence that polyphenol degradation is also of key importance for *E. polonica* infection and colonization of its woody host, Norway spruce. The direct correlation between the *in vitro* growth rate of *E. polonica* strains on astringin and catechin as sole carbon source and their virulence during spruce bark infection shows the importance of polyphenol degradation in nutrient acquisition. However, since these substances also are known as potent phytoalexins and phytoanticipins in other plant-pathogen interactions, it is likely that their catabolism functions at least in part as a detoxification mechanism. As *E. polonica* colonizes lignified bark and wood, polyphenol degradation also may serve to help gain entry into woody tissue. EpCDO4 may be especially important in this regard, as it is localized in the extracellular space and utilizes the lignin precursor caffeic acid at a higher efficiency than other spruce polyphenols.

E. polonica and other blue-stain fungi are commonly thought to play an important role in tree colonization by the European spruce bark beetle *I. typographus* by exhausting the spruce tree's chemical defense mechanisms (Krokene and Solheim, 1998, 2001; Nagy et al., 2004; Franceschi et al., 2005; Zhao et al., 2011). Although this opinion is not universally accepted (Six and Wingfield, 2011), our data suggest that polyphenol degradation could remove potentially harmful chemicals from the food of bark beetle larvae. Polyphenols are known to be antinutritional compounds that can form reactive quinones that react with constituents of insect cells (Barbehenn et al., 2008) and can precipitate proteins, making them inaccessible for digestion (Scalbert, 1991). The nutritional benefits associated with polyphenol biotransformation by *E. polonica*, therefore, might not only benefit the fungus but might drive the mutualistic interaction with its vector, *I. typographus*.

MATERIALS AND METHODS

Inoculation of Norway Spruce Saplings with *E. polonica*

Two *Endoconidiophora polonica* isolates (CMW 7749 = AV and CMW 7135 = V) provided by the culture collection of the Forestry and Agricultural Biotechnology Institute, University of Pretoria, were grown on 2% (w/v) malt extract agar (Carl Roth) for 12 d at 25°C in the dark.

Twelve-year-old Norway spruce (*Picea abies*) saplings originating from the 3369-Schongau clone (Samenklänge und Pflanzengarten) were grown in an outdoor plot for 8 years prior to the experiment. Inoculations of saplings with *E. polonica* were performed 3 weeks after their spring flush. A bark plug, 8 mm in diameter, was removed between the second and third branch whorl from the upper part of the sapling with a cork borer. An 8-mm plug from one of the two *E. polonica* cultures was placed into the wound with the mycelium oriented toward the wood surface and sealed with Parafilm. For the wounded control treatment, bark plugs were removed and a plug of sterile malt extract agar was inserted into the wound.

Bark tissue samples from inoculated and wounded control saplings were harvested 28 d after the onset of the experiment. The fungal lesions were separated into two parts: the inner lesion close to the inoculation point (about

18 mm²) and the expanding outer lesion (pooled sample). Five replicate trees were used for each treatment (inoculated with AV, inoculated with V, and wounded control). Lesion sections were flash frozen immediately after harvest in liquid nitrogen and stored at -80°C.

Quantitative Real-Time PCR of Plant and Fungal Transcripts

Total RNA from the inner and outer lesions and from wounded but uninoculated control bark was isolated with the Invitrap Spin Plant RNA Mini Kit (Stratagene) following the protocols of the manufacturer except that an additional DNA digestion step was included (RNase Free DNase set; Qiagen). RNA was quantified by spectrophotometry. Reverse transcription of 1 µg of RNA into complementary DNA (cDNA) was achieved using SuperScript II reverse transcriptase (Invitrogen) and 50 pmol of PolyT₁₂ primer (Invitrogen) in a reaction volume of 20 µL. After cDNA was diluted to 10% (v/v) with deionized water, 1 µL of diluted cDNA was used as a template for quantitative real-time PCR in a reaction mixture containing Brilliant SYBR Green QRT-PCR Master Mix (Stratagene) and 10 pmol of forward and 10 pmol of reverse primers. Primer sequences for *PaSTS*, *PaCHS*, and *EpCDO1* to *EpCDO4* are given in Supplemental Table S2. PCR was performed using a Stratagene MX3000P thermocycler using the following cycling parameters: 5 min at 95°C, followed by 40 cycles of 30 s at 95°C, 30 s at 55°C, and 30 s at 72°C, followed by a melting curve analysis from 55°C to 95°C. Reaction controls included nontemplate controls as well as non-reverse-transcribed RNA.

The primer pair chosen for *PaSTS* amplified transcripts of both orthologous transcripts present in the Norway spruce genome (for description, see Hammerbacher et al., 2011). The primer pair designed for *PaCHS* could amplify seven of the nine unique CHS transcripts identified in spruce (Hammerbacher et al., 2014). The transcript abundances of *PaSTS* and *PaCHS* were normalized to the transcript abundance of the ubiquitin transcript (primers in Supplemental Table S2; verified by Schmidt et al., 2010) and were calculated from three technical replicates each of five biological replicates. Relative transcript abundance was calibrated against the transcript abundance of five nonwounded control saplings.

The transcript abundance of *EpCDO* genes was normalized to the transcript abundance of the *E. polonica* CHITIN SYNTHASE1 transcript (primers in Supplemental Table S2) and was calculated from three technical replicates of five biological replicates. Relative transcript abundance was calibrated against the transcript abundance of a single replicate from an expanding lesion produced by V. The stability of the normalizing transcript was assessed by the amplification of eight normalizing transcript candidates using cDNA derived from *E. polonica* grown under different conditions and analysis of the results using the program GNorm (<https://genorm.cmgg.be>). The average expression stability for chitin synthase was calculated to be 0.145.

Extraction of Phenolic Compounds from Spruce

For the extraction of phenolic compounds, Norway spruce tissue was ground to a fine powder in liquid nitrogen and lyophilized at 0.34 mbar pressure using an Alpha 1-4 LD Plus freeze dryer (Martin Christ). Approximately 20 mg of dried tissue was extracted for 4 h at 4°C with 1 mL of analytical grade methanol containing 100 µg mL⁻¹ apigenin-7-glucoside (Carl Roth) as an internal standard. The extract was centrifuged at 3,200g, and the supernatant was recovered. Insoluble material was reextracted with 0.8 mL of methanol for 16 h. Supernatants were combined and analyzed directly by LC-MS.

Analysis of Phenolic Compounds by LC-MS with Electrospray Ionization

Phenolic compounds from spruce were separated on a Nucleodur Sphinx RP18ec column with dimensions of 250 × 4.6 mm and a particle size of 5 µm (Macherey-Nagel) using an Agilent 1100 series HPLC device (Agilent Technologies) with a flow rate of 1 mL min⁻¹. The column temperature was maintained at 25°C. Phenolic compounds were separated using 0.2% (v/v) formic acid and acetonitrile as mobile phases A and B, respectively, with the following elution profile: 0 to 1 min, 100% A; 1 to 25 min, 0% to 65% B in A; 25 to 28 min, 100% B; and 28 to 32 min, 100% A.

Compound detection and quantification was accomplished with an Esquire 6000 ESI ion-trap mass spectrometer (Bruker Daltonics). Flow coming from the column was diverted in a ratio of 4:1 before entering the mass spectrometer

electrospray chamber. Electrospray ionization-mass spectrometry was performed in negative mode scanning mass-to-charge ratio between 50 and 1,600 with an optimal target mass-to-charge ratio of 405. The mass spectrometer was operated using the following specifications: skimmer voltage, 60 V; capillary voltage, 4,200 V; nebulizer pressure, 35 p.s.i.; drying gas, 11 L min⁻¹; and gas temperature, 330°C. Capillary exit potential was kept at -121 V.

Compounds were identified by fragmentation patterns and by direct comparison of retention time and mass spectrum with those of available commercial standards, including 2,3-trans(+)-catechin, proanthocyanidin B1, taxifolin, and piceid (Sigma). Bruker Daltonics Quant Analysis version 3.4 software was used for data processing and compound quantification using a standard smoothing width of 3 and Peak Detection Algorithm version 2. Linearity in ionization efficiencies was verified by analyzing serial dilutions of randomly selected samples. An external calibration curve created by linear regression was used for the quantification of 2,3-trans(+)-catechin (Sigma) and astringin. All quantifications were adjusted relative to the signal for the internal standard.

Large-Scale Isolation of Astringin from Spruce Bark

Astringin was isolated by extracting 500 g of dried spruce bark ground to a fine powder with methanol. The methanol was evaporated completely, and the extract was partially solubilized in 100 mL of water using an ultrasonic water bath and filtered. A portion (20 mL) of the aqueous solution was loaded on a Sephadex LH20 (GE Healthcare) column with dimensions of 2.5 cm × 30 cm. The compounds were eluted from the column using water at a flow speed of 1 mL min⁻¹. Fractions (15 mL) were collected and analyzed for astringin content by direct injection into a mass spectrometer using an autosampler from an Agilent 1200 HPLC system (Agilent Technologies) coupled to an API 3200 tandem mass spectrometer (Applied Biosystems) equipped with a turbospray ion source operating in negative ionization mode. Injection volume was 5 μL using flow injection analysis. The mobile phase consisted of 0.05% formic acid (A) and acetonitrile (B) utilizing a flow of 1 mL min⁻¹. Phase A was maintained at 50% for 0.5 min. The ion spray voltage was maintained at -4.5 keV. The turbo gas temperature was set at 600°C. Nebulizing gas was set at 50 p.s.i., curtain gas at 30 p.s.i., heating gas at 60 p.s.i., and collision gas at 5 p.s.i. Multiple reaction monitoring was used to monitor analyte parent ion → product ion as described in Supplemental Table S1. Pure fractions were pooled and lyophilized using a freeze dryer.

Fungal Biotransformation of Catechin and Astringin

Fungal isolates V and AV were grown on potato dextrose agar in petri dishes for 7 d. Agar plugs (2 mm diameter) from these cultures were inoculated into 2 mL of potato dextrose broth containing astringin or catechin (Sigma; 1 mg mL⁻¹). After 12 h, the liquid broth of the fungal cultures was sampled and analyzed by liquid chromatography-electrospray ionization-tandem mass spectrometry (LC-ESI-MS/MS) for astringin and catechin as well as catabolites of these compounds. Five replicates were used per treatment. Controls included fungal cultures treated with water instead of the phenolic compounds as well as sterile medium containing astringin or catechin.

LC-ESI-MS/MS of Fungal Biotransformation Products of Astringin and Catechin

Chromatography was performed on an Agilent 1200 HPLC system (Agilent Technologies). Separation was achieved on a 100- × 4.6-mm Kinetex C18 column with particle size of 2.6 μm (Phenomenex). Formic acid (0.05%) in water and acetonitrile were employed as mobile phases A and B, respectively. The elution profile was as follows: 0 to 1 min, 100% A; 1 to 7 min, 0% to 65% B in A; 7 to 8 min, 65% to 100% B in A; 8 to 9 min, 100% B; and 9 to 10 min, 100% A. The total mobile phase flow rate was 1.5 mL min⁻¹. The column temperature was maintained at 25°C.

An API 3200 tandem mass spectrometer (Applied Biosystems) equipped with a Turbospray ion source was operated in negative ionization mode. The instrument parameters were optimized by infusion experiments with pure standards of catechin, catechin lactone, astringin, piceatannol, and astringin muconate. The ion spray voltage was maintained at -4,500 V. The turbo gas temperature was set at 700°C. Nebulizing gas was set at 70 p.s.i., curtain gas at 25 p.s.i., heating gas at 60 p.s.i., and collision gas at 10 p.s.i. Multiple reaction monitoring was used to monitor analyte precursor ion → product ion as described in Supplemental Table S1. Both Q1 and Q3 quadrupoles were

maintained at unit resolution. Analyst 1.5 software (Applied Biosystems) was used for data acquisition and processing. The linearity of compound detection for quantification was verified by external calibration curves for catechin and astringin.

E. polonica EST Sequencing, Assembly, and Identification of *EpCDO* Transcripts

Cultures of *E. polonica* AV and V were grown in liquid medium for 7 d, after which 1 mM astringin or catechin was added to the medium. Cultures were incubated for a further 24 h and harvested by centrifugation. Mycelium was freeze dried, and RNA was extracted using the method described by Kolosova et al. (2004). The integrity of the RNA was verified using an Agilent 2100 Bioanalyzer and an RNA 6000 Nano Kit (Agilent Technologies). The quantity of RNA was determined using a Nanodrop ND-1000 spectrophotometer. The quality of RNA was assessed by spectrophotometry as well as by bioanalyzer. Samples from both isolates as well as from the catechin and astringin treatments were pooled to obtain a single sample. Library generation and sequencing were carried out by Eurofins MWG Operon (www.eurofinsgenomics.eu) using the Illumina HiSeq 2000 platform. Quality control included filtering high-quality reads based on the fastq score and trimming the read lengths using CLC Genomics Workbench software version 5.0.1 (<http://www.clcbio.com>). After these filtering steps, the Illumina reads were assembled de novo using CLC Genomics Workbench software version 5.0.1 according to described procedures (Vogel et al., 2014).

Protein CDO sequences from *Ophiostoma piceae* (Haridas et al., 2013) and *Grosmannia clavigera* (DiGuistini et al., 2011) were used to screen our *E. polonica* EST collection for candidate cDNA sequences using tBLASTn. Searches yielded one full-length and three partial open reading frames for putative CDO genes. Full-length transcripts for three CDOs were generated by RACE using the Clontech kit (BD Biosciences) following the manufacturer's protocols. Open reading frames from candidate sequences were detected manually using the software package DNA Star version 8.02 (DNASTAR), and the absence/presence of predicted signal peptides at the N terminus was confirmed by SignalP software (<http://www.cbs.dtu.dk/services>).

Cloning and Sequence Analysis *EpCDO* Transcripts

For RNA purification, mycelium from 7-d-old liquid cultures was used according to the method developed by Kolosova et al. (2004). One microgram of total RNA was converted to cDNA in a 20-μL reverse transcription reaction using SuperScript II reverse transcriptase (Invitrogen) and 50 pmol of PolyT₍₁₂₋₁₈₎ primer (Invitrogen). Primers (Supplemental Table S2) were designed for candidate sequences using the N- and C-terminal sequences of four putative CDO transcripts (Gateway [Invitrogen] compatible) identified in our *E. polonica* EST library. Pseudomature forms of *EpCDO* cDNA were PCR amplified with primers using Platinum Taq high-fidelity DNA polymerase (Invitrogen) and purified with the QIAquick PCR purification kit (Qiagen). Gateway entry clones were made using BP Clonase II and pDONR207 (Invitrogen) following the manufacturer's protocol. pDONR207 constructs containing *EpCDO* transcripts were Sanger sequenced using 10 pmol of transcript-specific primer and the BigDye Terminator version 3.1 Cycle Sequencing Kit on an ABI Prism R 3100 sequencing system (Applied Biosystems). Sequences from each construct were assembled and translated into protein sequence using DNA Star software.

Phylogenetic Analysis of CDO Proteins in Blue-Stain Fungi

Proteomes of *G. clavigera* kw1407 and *O. piceae* UAMH 11346 were downloaded from the National Center for Biotechnology Information (www.ncbi.nlm.nih.gov). The proteome of *Ophiostoma novo-ulmi* was downloaded from the supplementary data of Comeau et al. (2015). Ophiostomatoid proteomes were mined with HMMER version 3.1b1, using profile hmms for Dioxygenase_C (Pfam identifier PF00775), Dioxygenase_N (Pfam identifier PF04444), and LigB domains (Pfam identifier PF02900) from the Pfam database (<http://pfam.xfam.org>; Finn et al., 2011) as queries. Retrieved CDO protein sequences from all four blue-stain fungi were aligned with MAFFT (Katoh et al., 2002). The WAG fixed-rate model of amino acid substitution and γ -distributed rates across sites were selected according to the Aikake and Bayesian information criteria using modelGenerator version 0.851 (Keane et al., 2006). The phylogeny was constructed using MrBayes version 3.2.5 (Ronquist et al., 2012). MCMC searches

were conducted with the WAG+G evolutionary model and default prior settings for 2,000,000 generations with a sample frequency of 200 and a relative burn-in fraction of 30%. The convergence of the log-likelihood values of the trees was examined via the average SD of split frequencies.

Heterologous Expression of *EpCDO* Transcripts in *Escherichia coli*

Four putative *EpCDO* pDONR207 constructs were cloned with LR Clonase II (Invitrogen) according to the manufacturer's instructions into the Gateway-compatible expression vector pH9GW (Yu and Liu, 2006), which contains nine His residues 5' of the N terminus of the expressed protein. All constructs were verified by sequencing. Arctic Express (DE3) chemically competent *E. coli* (Stratagene), which coexpresses cold-adapted chaperonins to overcome protein misfolding and insolubility, was transformed with the expression constructs. For protein expression, single colonies were inoculated into 5 mL of Luria-Bertani broth with 1 $\mu\text{g mL}^{-1}$ kanamycin and grown for 16 h at 24°C. The 5-mL starter cultures were used to inoculate 100 mL of Overnight Express Instant TB Medium (Novagen) supplemented with 1% (v/v) glycerol and 1 $\mu\text{g mL}^{-1}$ kanamycin.

Bacterial cultures were grown for 3 d at 12°C (220 rpm) and harvested by centrifugation. Bacteria were resuspended in 10 mL of buffer containing 50 mM Tris (pH 7), 10% (v/v) glycerol, 0.5 mM phenylmethylsulfonyl fluoride, and 1 mM DTT and lysed by sonification for 3 min using two cycles at 65% power with a Bandelin Sonoplus HD 2070 sonicator (Bandelin Electronics). Insoluble cell debris was removed from the lysate by centrifugation at 16,000g for 30 min at 4°C.

Expressed proteins were purified from the crude lysate by affinity chromatography with a 1-mL His Trap FF column (GE Healthcare Life Sciences) on an AEKTA 900 chromatography system (GE Healthcare) using a wash buffer containing 50 mM Tris (pH 7), 25 mM imidazole, and 10% (v/v) glycerol. His-tagged proteins were eluted from the column with wash buffer amended with 250 mM imidazole. Fractions containing the expressed proteins were desalted into an assay buffer (50 mM Bis-Tris, pH 7.5, 10% [v/v] glycerol, and 1 mM DTT) on DG-10 desalting columns (Bio-Rad) and stored at 4°C. The protein concentration was determined using the Bradford reagent (Bio-Rad).

In Vitro Functional Characterization and Kinetics of *EpCDO* Expressed in *E. coli*

Substrates (Table II) were purchased from Sigma or, in the case of astringin, purified on a Sephadex LH20 column (the purification procedure is described above). Recombinant CDO1 to CDO4 enzyme activities were assayed in 200- μL reaction volumes containing 1.9 μg of purified enzyme, 0.005 mM $\text{FeCl}_3/\text{FeCl}_2$, and 10 mM phenolic substrate in assay buffer. Reaction mixtures were incubated for 15 min at 30°C before the enzyme assay was stopped by acidification with 10 μL of 0.1 N HCl. Negative control assays were initiated without substrate or with heat-denatured enzyme preparations. The temperature optimum for CDO activity was determined by incubating assays at 25°C, 30°C, and 35°C; optimum pH between pH 6 and 8.5 and cofactor concentrations between 0.01 and 2 mM were tested. Assay products were analyzed by LC-ESI-MS/MS as described above.

Kinetic data were recorded in experiments where only one of the phenolic substrates was varied. V_{max} , k_{cat} , and K_m values for phenolic substrates were determined using 0.001 to 10 mM substrate in air-saturated buffer. Kinetic data were calculated from the initial velocities using the Michaelis-Menten equation by nonlinear regression using Sigma Plot software (Systat Software).

Pathogenicity Assay

Eight *E. polonica* isolates (CMW 7135, 7140, 7143, 7146, 7152, 7749, 8830, and 1993-208/115; Krokene and Solheim, 1998) were cultured on 20% (v/v) carrot (*Daucus carota*) agar at 25°C in darkness for 1 week. Four-year-old potted *Picea glauca* saplings (60 cm) were inoculated at a stem height of 20 cm by separating a bark plug from the wood with a 6-mm cork borer. A similarly sized *E. polonica* inoculum plug with mycelium orientated toward the wood was placed in the wound and sealed with Parafilm. Sterile 20% (v/v) carrot juice agar was used as a negative control. Plants were maintained in a growth chamber (16 h of light, 24°C, and 70% relative humidity) for 4 weeks. Bark tissues from treatment and control plants were separated from wood, and the fungal lesions were measured at the bark surface. Since there were large differences in the virulence of the fungi, the lesion lengths were converted into rank values.

To confirm that virulence was similar in both spruce species, Norway spruce and *P. glauca*, lesion lengths induced by AV and V inoculation in both species were plotted against each other. We found that *E. polonica* could infect both species but that lesion lengths were larger in Norway spruce. However, a clear correlation between lesion lengths in Norway spruce and *P. glauca* was observed ($r^2 = 0.94$; Supplemental Fig. S1), leading to the assumption that relative virulence also could be estimated using *P. glauca* as a host.

Fungal Growth on Catechin and Astringin

To determine fungal growth on catechin and astringin, the growth medium was prepared by steam sterilizing synthetic nutrient agar (Nirenberg and O'Donnell, 1998) and adding filter-sterilized astringin or catechin to a concentration of 1 mM. Medium was dispensed in petri dishes (5.2 cm diameter). After the medium solidified, an agar plug (4 mm diameter) from a 10-d-old *E. polonica* stationary culture was placed in the middle of each petri dish, sealed with Parafilm, and incubated at 26°C in the dark. Fungal growth was measured every 24 h until growth reached the margins of the petri dish.

Statistical Analysis

All statistical analyses were conducted using R (www.r-project.org). A multivariate repeated-measures model was used to calculate differences between analytes and transcript abundances in fungus-infested lesion sections. Biotransformation efficiency was analyzed using the nonparametric Kruskal-Wallis test. Pathogenicity was analyzed using a one-way ANOVA. Fungal growth on petri dishes was analyzed using linear regression. Differences in mean fungal growth rate were calculated using a two-way ANOVA followed by Tukey's posthoc test. Correlations between virulence and growth on carbon sources were calculated using nonlinear regressions.

Sequence data from this article can be found in the GenBank/EMBL data libraries under accession numbers KU221039, KU221040, KU221041, and KU221042.

Supplemental Data

The following supplemental materials are available.

Supplemental Figure S1. Correlation between lesion lengths created by *E. polonica* in Norway spruce and *P. glauca*.

Supplemental Table S1. Mass spectral parameters for the analysis of selected molecules.

Supplemental Table S2. Primer sequences for quantitative PCR and cloning.

ACKNOWLEDGMENTS

We thank Bettina Raguschke for assistance in the laboratory, Michael Reichelt for additional training on the analytical equipment, Michael Wingfield for supplying the *E. polonica* cultures, and Axel Schmidt for supplying the *P. glauca* trees for the pathogenicity assays.

Received December 7, 2015; accepted April 19, 2016; published April 22, 2016.

LITERATURE CITED

- Adrian M, Rajaei H, Jeandet P, Veneau J, Bessis R (1998) Resveratrol oxidation in *Botrytis cinerea* conidia. *Phytopathology* **88**: 472–476
- Barbehenn RV, Maben RE, Knoester JJ (2008) Linking phenolic oxidation in the midgut lumen with oxidative stress in the midgut tissues of a tree-feeding caterpillar *Malacosoma disstria* (Lepidoptera: Lasiocampidae). *Environ Entomol* **37**: 1113–1118
- Brignolas F, Lacroix B, Lieutier F, Sauvard D, Drouet A, Claudot AC, Yart A, Berryman AA, Christiansen E (1995) Induced responses in phenolic metabolism in two Norway spruce clones after wounding and inoculations with *Ophiostoma polonicum*, a bark beetle-associated fungus. *Plant Physiol* **109**: 821–827
- Chen HP, Chow M, Liu CC, Lau A, Liu J, Eltis LD (2012) Vanillin catabolism in *Rhodococcus jostii* RHA1. *Appl Environ Microbiol* **78**: 586–588

- Chen Z, Liang J, Zhang C, Rodrigues CJ Jr (2006) Epicatechin and catechin may prevent coffee berry disease by inhibition of appressorial melanization of *Colletotrichum kahawae*. *Biotechnol Lett* **28**: 1637–1640
- Cheynier V (2012) Phenolic compounds: from plants to foods. *Phytochem Rev* **11**: 153–177
- Chong JL, Poutaraud A, Huguene P (2009) Metabolism and roles of stilbenes in plants. *Plant Sci* **177**: 143–155
- Comeau AM, Dufour J, Bouvet GF, Jacobi V, Nigg M, Henrissat B, Laroche J, Levesque RC, Bernier L (2015) Functional annotation of the *Ophiostoma novo-ulmi* genome: insights into the phytopathogenicity of the fungal agent of Dutch elm disease. *Genome Biol Evol* **7**: 410–430
- Dashtban M, Schraft H, Qin W (2009) Fungal bioconversion of lignocellulosic residues: opportunities & perspectives. *Int J Biol Sci* **5**: 578–595
- de Beer ZW, Duong TA, Barnes I, Wingfield BD, Wingfield MJ (2014) Redefining *Ceratocystis* and allied genera. *Stud Mycol* **79**: 187–219
- DiGiustini S, Wang Y, Liao NY, Taylor G, Tanguay P, Feau N, Henrissat B, Chan SK, Hesse-Orce U, Alamouti SM, et al (2011) Genome and transcriptome analyses of the mountain pine beetle-fungal symbiont *Grosmannia clavigera*, a lodgepole pine pathogen. *Proc Natl Acad Sci USA* **108**: 2504–2509
- El Hadrami A, Islam MR, Adam LR, Daayf F (2015) A cupin domain-containing protein with a quercetinase activity (VdQase) regulates *Verticillium dahliae*'s pathogenicity and contributes to counteracting host defenses. *Front Plant Sci* **6**: 440
- Finn RD, Clements J, Eddy SR (2011) HMMER web server: interactive sequence similarity searching. *Nucleic Acids Res* **39**: W29–W37
- Franceschi VR, Krokene P, Christiansen E, Krekling T (2005) Anatomical and chemical defenses of conifer bark against bark beetles and other pests. *New Phytol* **167**: 353–375
- Gall DL, Ralph J, Donohue TJ, Noguera DR (2014) A group of sequence-related sphingomonad enzymes catalyzes cleavage of β -aryl ether linkages in lignin β -guaiaacyl and β -syringyl ether dimers. *Environ Sci Technol* **48**: 12454–12463
- Gan P, Ikeda K, Irieda H, Narusaka M, O'Connell RJ, Narusaka Y, Takano Y, Kubo Y, Shirasu K (2013) Comparative genomic and transcriptomic analyses reveal the hemibiotrophic stage shift of *Colletotrichum* fungi. *New Phytol* **197**: 1236–1249
- Gulvik CA, Buchan A (2013) Simultaneous catabolism of plant-derived aromatic compounds results in enhanced growth for members of the *Roseobacter* lineage. *Appl Environ Microbiol* **79**: 3716–3723
- Haigler BE, Pettigrew CA, Spain JC (1992) Biodegradation of mixtures of substituted benzenes by *Pseudomonas* sp. strain JS150. *Appl Environ Microbiol* **58**: 2237–2244
- Hammerbacher A, Paetz C, Wright LP, Fischer TC, Bohlmann J, Davis AJ, Fenning TM, Gershenzon J, Schmidt A (2014) Flavan-3-ols in Norway spruce: biosynthesis, accumulation, and function in response to attack by the bark beetle-associated fungus *Ceratocystis polonica*. *Plant Physiol* **164**: 2107–2122
- Hammerbacher A, Ralph SG, Bohlmann J, Fenning TM, Gershenzon J, Schmidt A (2011) Biosynthesis of the major tetrahydroxystilbenes in spruce, astringin and isorhapontin, proceeds via resveratrol and is enhanced by fungal infection. *Plant Physiol* **157**: 876–890
- Hammerbacher A, Schmidt A, Wadke N, Wright LP, Schneider B, Bohlmann J, Brand WA, Fenning TM, Gershenzon J, Paetz C (2013) A common fungal associate of the spruce bark beetle metabolizes the stilbene defenses of Norway spruce. *Plant Physiol* **162**: 1324–1336
- Haridas S, Wang Y, Lim L, Massoumi Alamouti S, Jackman S, Docking R, Robertson G, Birol I, Bohlmann J, Breuil C (2013) The genome and transcriptome of the pine saprophyte *Ophiostoma piceae*, and a comparison with the bark beetle-associated pine pathogen *Grosmannia clavigera*. *BMC Genomics* **14**: 373
- Harwood CS, Parales RE (1996) The beta-ketoadipate pathway and the biology of self-identity. *Annu Rev Microbiol* **50**: 553–590
- Katoh K, Misawa K, Kuma K, Miyata T (2002) MAFFT: a novel method for rapid multiple sequence alignment based on fast Fourier transform. *Nucleic Acids Res* **30**: 3059–3066
- Kausrud K, Økland B, Skarpaas O, Grégoire JC, Erbilgin N, Stenseth NC (2012) Population dynamics in changing environments: the case of an eruptive forest pest species. *Biol Rev Camb Philos Soc* **87**: 34–51
- Keane TM, Creevey CJ, Pentony MM, Naughton TJ, McInerney JO (2006) Assessment of methods for amino acid matrix selection and their use on empirical data shows that ad hoc assumptions for choice of matrix are not justified. *BMC Evol Biol* **6**: 29
- Keeling CI, Bohlmann J (2006) Genes, enzymes and chemicals of terpenoid diversity in the constitutive and induced defence of conifers against insects and pathogens. *New Phytol* **170**: 657–675
- Kirisits T (2010) Fungi isolated from *Picea abies* infested by the bark beetle *Ips typographus* in the Bialowieza forest in north-eastern Poland. *For Pathol* **40**: 100–110
- Kolossova N, Miller B, Ralph S, Ellis BE, Douglas C, Ritland K, Bohlmann J (2004) Isolation of high-quality RNA from gymnosperm and angiosperm trees. *Biotechniques* **36**: 821–824
- Krokene P, Solheim H (1998) Pathogenicity of four blue-stain fungi associated with aggressive and nonaggressive bark beetles. *Phytopathology* **88**: 39–44
- Krokene P, Solheim H (2001) Loss of pathogenicity in the blue-stain fungus *Ceratocystis polonica*. *Plant Pathol* **50**: 497–502
- Kuroda K (2005) Xylem dysfunction in Yezo spruce (*Picea jezoensis*) after inoculation with the blue-stain fungus *Ceratocystis polonica*. *For Pathol* **35**: 346–358
- Li SH, Nagy NE, Hammerbacher A, Krokene P, Niu XM, Gershenzon J, Schneider B (2012) Localization of phenolics in phloem parenchyma cells of Norway spruce (*Picea abies*). *ChemBioChem* **13**: 2707–2713
- Lowe TM, Ailloud F, Allen C (2015) Hydroxycinnamic acid degradation, a broadly conserved trait, protects *Ralstonia solanacearum* from chemical plant defenses and contributes to root colonization and virulence. *Mol Plant Microbe Interact* **28**: 286–297
- Martin D, Tholl D, Gershenzon J, Bohlmann J (2002) Methyl jasmonate induces traumatic resin ducts, terpenoid resin biosynthesis, and terpenoid accumulation in developing xylem of Norway spruce stems. *Plant Physiol* **129**: 1003–1018
- Nagy NE, Fossdal CG, Krokene P, Krekling T, Lönneborg A, Solheim H (2004) Induced responses to pathogen infection in Norway spruce phloem: changes in polyphenolic parenchyma cells, chalcone synthase transcript levels and peroxidase activity. *Tree Physiol* **24**: 505–515
- Nirenberg HI, O'Donnell K (1998) New *Fusarium* species and combinations within the *Gibberella fujikuroi* species complex. *Mycologia* **90**: 434–458
- Paine TD, Raffa KF, Harrington TC (1997) Interactions among Scolytid bark beetles, their associated fungi, and live host conifers. *Annu Rev Entomol* **42**: 179–206
- Pillai BVS, Swarup S (2002) Elucidation of the flavonoid catabolism pathway in *Pseudomonas putida* PML2 by comparative metabolic profiling. *Appl Environ Microbiol* **68**: 143–151
- Pont V, Pezet R (1990) Relation between the chemical structure and the biological activity of hydroxystilbenes against *Botrytis cinerea*. *J Phytopathol* **130**: 1–8
- Ronquist F, Teslenko M, van der Mark P, Ayres DL, Darling A, Höhna S, Larget B, Liu L, Suchard MA, Huelsenbeck JP (2012) MrBayes 3.2: efficient Bayesian phylogenetic inference and model choice across a large model space. *Syst Biol* **61**: 539–542
- Scalbert A (1991) Antimicrobial properties of tannins. *Phytochemistry* **30**: 3875–3883
- Schiebe C, Hammerbacher A, Birgersson G, Witzell J, Brodelius PE, Gershenzon J, Hansson BS, Krokene P, Schlyter F (2012) Inducibility of chemical defenses in Norway spruce bark is correlated with unsuccessful mass attacks by the spruce bark beetle. *Oecologia* **170**: 183–198
- Schmidt A, Wächter B, Temp U, Krekling T, Séguin A, Gershenzon J (2010) A bifunctional geranyl and geranylgeranyl diphosphate synthase is involved in terpene oleoresin formation in *Picea abies*. *Plant Physiol* **152**: 639–655
- Six DL, Wingfield MJ (2011) The role of phytopathogenicity in bark beetle-fungus symbioses: a challenge to the classic paradigm. *Annu Rev Entomol* **56**: 255–272
- Suenaga H, Koyama Y, Miyakoshi M, Miyazaki R, Yano H, Sota M, Ohtsubo Y, Tsuda M, Miyazaki K (2009) Novel organization of aromatic degradation pathway genes in a microbial community as revealed by metagenomic analysis. *ISME J* **3**: 1335–1348
- Vaillancourt FH, Bolin JT, Eltis LD (2006) The ins and outs of ring-cleaving dioxygenases. *Crit Rev Biochem Mol Biol* **41**: 241–267

- Viiri H, Annala E, Kitunen V, Niemelä P** (2001) Induced responses in stilbenes and terpenes in fertilized Norway spruce after inoculation with blue-stain fungus, *Ceratocystis polonica*. *Trees* **15**: 112–122
- Vogel H, Badapanda C, Knorr E, Vilcinskas A** (2014) RNA-sequencing analysis reveals abundant developmental stage-specific and immunity-related genes in the pollen beetle *Meligethes aeneus*. *Insect Mol Biol* **23**: 98–112
- Wang Y, Lim L, Madilao L, Lah L, Bohlmann J, Breuil C** (2014) Gene discovery for enzymes involved in limonene modification or utilization by the mountain pine beetle-associated pathogen *Grosmannia clavigera*. *Appl Environ Microbiol* **80**: 4566–4576
- Wermelinger B** (2004) Ecology and management of the spruce bark beetle *Ips typographus*: a review of recent research. *For Ecol Manage* **202**: 67–82
- Yu XH, Liu CJ** (2006) Development of an analytical method for genome-wide functional identification of plant acyl-coenzyme A-dependent acyltransferases. *Anal Biochem* **358**: 146–148
- Zhao T, Krokene P, Hu J, Christiansen E, Björklund N, Långström B, Solheim H, Borg-Karlson AK** (2011) Induced terpene accumulation in Norway spruce inhibits bark beetle colonization in a dose-dependent manner. *PLoS ONE* **6**: e26649

Supplemental Data

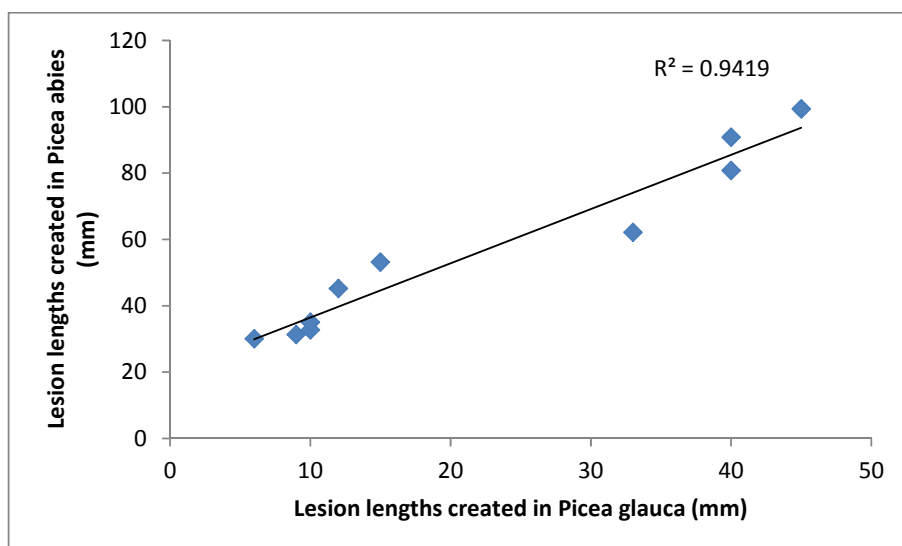


Figure S1: Correlation between lesion lengths created by *E. polonica* in *P. abies* and *P. glauca*.

Table S1: Mass spectral parameters for the analysis of selected molecules (Q1, First quadrupole; Q2, second quadrupole; DP, declustering potential; EP, entrance potential; CEP, cell entrance potential; CE, collision energy; CXP, cell exit potential).

Q1 (mass)	Q2 (mass)	Compound	DP	EP	CEP	CE	CXP
108.9	91.1	Catechol	-35	-8	-10.0	-24	-2
321.338	232.951	Catechin muconolactone	-40	-4	-18.0	-20	-6
140.8	97	Catechol muconolactone	-13	-2	-7.0	-9	-1
178.923	134.854	Caffeic acid	-30	-11	-16.0	-20	-10
210.847	122.91	Caffeic acid muconolactone	-375	-4.5	-14.0	-14	-2
404.8	243	Astringin	-50	-5	-33.8	-38	-4
288.9	109	Catechin	-30	-10	-30.7	-34	0
436.9	230.8	Astringin muconolactone	-195	-4.5	-18.0	-32	-4
302.8	125.1	Taxifolin	-40	-9	-31.1	-28	0
304.9	125	Gallocatechin	-30	-10.5	-31.1	-28	-2
418.9	257.1	Isorhapontin	-25	-4.5	-34.2	-18	-4
576.9	289.1	ProanthocyanidinB1	-50	-9	-38.5	-30	-4
465	285	Taxifolin glucoside	-55	-4.5	-35.4	-44	-3
353	191	Clorogenic acid	-25	-4	-12.0	-24	-4

Table S2: Primer sequences for QPCR and cloning

Primer	Application	Sequence (5' -> 3')
<i>Pa</i> STS F	QPCR	GTGGCGAGCAGAACACAGACTTC
<i>Pa</i> STS R	QPCR	CAGCGATGGTACCTCCATGAACG
<i>Pa</i> CHS F	QPCR	CAGCAGTTCGGAATCTCGGACTGGAAC
<i>Pa</i> CHS R	QPCR	CTCATCTCGTCCAAGATGAAGTGCACGC
<i>Pa</i> UBI F	QPCR	GTTGATTTTTGCTGGCAAGC
<i>Pa</i> UBI R	QPCR	CACCTCTCAGACGAAGTAC
<i>Ep</i> CDO1 F	QPCR	CACTACAGAGGGTTCGGTGCTTGGC
<i>Ep</i> CDO1 R	QPCR	CGGAATCGGATAACTGACTGGTTTGATAC
<i>Ep</i> CDO2 F	QPCR	GATCTCACAATCGACAACATCACGCC
<i>Ep</i> CDO2 R	QPCR	CAGCGCCGTCATCCACTCCTCAGTAC
<i>Ep</i> CDO3 F	QPCR	CACTGCCCCGCCAGCCTCGTGC
<i>Ep</i> CDO3 R	QPCR	CCGTGATCCCAGCCTCTCTTAGCATC
<i>Ep</i> CDO4 F	QPCR	GCTCAAGGCTCGTGGTGTCACTGC
<i>Ep</i> CDO4 R	QPCR	GGAACGGGGGCAGGTCTCGACATC
<i>Ep</i> ChSy F	QPCR	CACGGTGATCACACACTGTCTGCG
<i>Ep</i> ChSy R	QPCR	CACAAGCTCGAAGCAGAGAATACGATC
<i>Ep</i> CDO1 F	Cloning	GW-F-adaptor-ATGGGCTCTCTTGTAACGTCGCC
<i>Ep</i> CDO1 R	Cloning	GW-R-adaptor-TTATTCAACTTCTGGAAGTGGAAAG
<i>Ep</i> CDO2 F	Cloning	GW-F-adaptor-ATGGCCGTCGAGACAGTCACTCTC
<i>Ep</i> CDO2 R	Cloning	GW-R-adaptor-TCAAGCAGCCACCTTCTTGTCGG
<i>Ep</i> CDO3 F	Cloning	GW-F-adaptor-ATGGTCAGAGCTCCCGTTGTCTGC
<i>Ep</i> CDO3 R	Cloning	GW-R-adaptor-CTAAGCGACTGGATCAGCTCCCC
<i>Ep</i> CDO4 F	Cloning	GW-F-adaptor-ATGGTCTTCGTTTCGCAACATCATC
<i>Ep</i> CDO4 R	Cloning	GW-R-adapt.-TTAGTAGGCAACACCACCAGACTC